AIP | Applied Physics Letters

Standoff explosives trace detection and imaging by selective stimulated Raman scattering

Marshall T. Bremer and Marcos Dantus

Citation: Appl. Phys. Lett. **103**, 061119 (2013); doi: 10.1063/1.4817248
View online: http://dx.doi.org/10.1063/1.4817248
View Table of Contents: http://apl.aip.org/resource/1/APPLAB/v103/i6
Published by the AIP Publishing LLC.

Standoff explosives trace detection and imaging by selective stimulated Raman scattering

Marshall T. Bremer[1] and Marcos Dantus[1,2,a)]
[1]*Department of Physics and Astronomy, Michigan State University, East Lansing, Michigan 48824, USA*
[2]*Department of Chemistry, Michigan State University, East Lansing, Michigan 48824, USA*

(Received 8 June 2013; accepted 8 July 2013; published online 9 August 2013)

We introduce a sensitive method for laser based standoff detection of chemicals based on stimulated Raman scattering. Selective excitation of a particular Raman transition is detected by measuring the diffusely reflected laser light from a distant surface. The method simultaneously measures stimulated Raman loss and gain within a single laser shot and is insensitive to the optical properties (reflectivity/absorptivity) of the substrate. We demonstrate the specificity and sensitivity by detecting and imaging nanogram analyte micro-crystals on paper, fabric, and plastic substrates at 1 to 10 m standoff distance using only 10 mW of laser power from a single femtosecond laser. © *2013 AIP Publishing LLC*. [http://dx.doi.org/10.1063/1.4817248]

Standoff detection of hazardous materials remains an important challenge which persists despite decades of research.[1–4] A key facet of this broad goal is the ability to safely and non-destructively detect, at modest standoff (2–20 m), trace quantities of explosives as indicators of concealed dangers in public spaces. Due to the low vapor pressure of most explosives,[2] an optical method capable of selectively detecting these compounds as microcrystals on different surfaces, including delicate garments, is highly desirable. The method introduced here has Raman chemical specificity, excellent sensitivity, and robust performance on virtually all surfaces.

Detecting minute quantities of condensed-phase hazards within the complex chemical background of real world surfaces requires exceptional chemical specificity. Raman spectroscopy provides unique chemical determination and the well separated, narrow features make it the preferred method in laser based identification of chemicals within complex environments. Raman has been used to identify bulk quantities of explosives at 50–500 m standoff,[5,6] and single microcrystals within fingerprints using a microscope.[7] However, the small spontaneous Raman cross-section has prevented standoff detection of trace quantities ($<100\,\mu g/cm^2$) within a few seconds.

Non-linear Raman spectroscopy in the form of coherent anti-Stokes Raman scattering (CARS) has been developed to enhance the signal of spontaneous Raman through coherent signal addition and applied to standoff detection.[8–13] Recently, single-beam CARS was used to detect $2\,\mu g/cm^2$ concentrations of an explosive simulant within a complex background at 1 m standoff within 1 s.[14] However, the analyte was deposited on ideal (specular) surfaces, and diffusive or absorbing substrates dramatically reduce the number of photons collected and therefore the sensitivity of the method. The Silberberg group subsequently used the non-resonant background for heterodyne amplification of the CARS signal, allowing detection of sub-milligram quantities of explosives deposited on absorbing substrates, at a distance of 50 m with $\sim 10^{-5}$ sr collection.[15] In this Letter, the intrinsically heterodyned stimulated Raman scattering signal is used to quickly detect and image sub-microgram quantities of explosives on real world substrates, with similar solid angle collection.

Stimulated Raman scattering (SRS) can be described as a third-order wave coupling process mediated by Raman transitions.[16] Phenomenologically, when a ground state molecule is in the presence of two strong fields, there is a transfer of photons from the high frequency field to the low frequency field if their frequency difference matches a Raman transition within a molecule. Conservation of energy is ensured by changes in the population of the excited vibrational state. This effect has been used to provide label free chemical contrast in microscopy,[17,18] achieving video rate imaging *in vivo*.[19] The most sensitive implementation requires two synchronized lasers, where >1 MHz rate intensity modulation of one beam is imprinted on the other beam and measured with lock-in amplification, nearly eliminating noise due to laser fluctuations.[20] The technique implemented here, which we call single-beam SRS (SB-SRS), includes several aspects, which are broadly of interest to the non-linear optics community. We use a *single* femtosecond laser and computer controlled pulse shaper to selectively excite a particular vibration through the SRS process. Macroscopic applications require low repetition-rate amplified lasers, which preclude MHz rate modulation. Instead, we create an intrinsic reference, a delayed replica pulse, which provides optimal measurement of stimulated Raman loss (SRL) and gain (SRG) at low repetition rates, even under single-shot operation. The reference has the same spectrum and intensity, allowing *simultaneous* measurement of SRL and SRG.

Figure 1 shows a schematic of the experiment. Details of the laser source, supercontinuum generation, and pulse shaper have been described previously.[9] The temporal profile of a broadband femtosecond laser pulse is modified, through spectral phase shaping, to excite a particular Raman mode. Multiphoton intrapulse interference phase scan (MIIPS) is used to correct for all dispersion in the setup before applying the calculated phase.[21] A time delayed reference pulse,

a)Author to whom correspondence should be addressed. Electronic mail: dantus@msu.edu

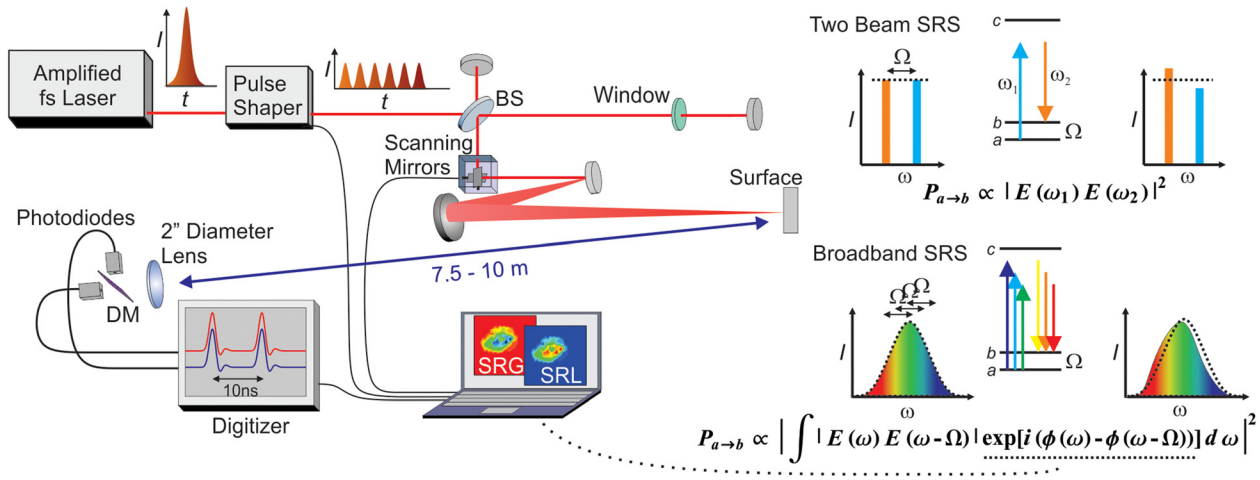

FIG. 1. Schematic of the SB-SRS experimental setup. The spectral phase of a broadband femtosecond laser is modified with a pulse shaper. A Michelson interferometer creates two collinear pulses. The window adds dispersion to the second pulse. The beam is steered by the fast scanning mirrors and expanded and focused at 1 m on the sample surface. A lens collects the diffusely reflected light at a distance of 7.5–10 m. The signal is split between two fast photodiodes using a dichroic mirror and digitized with an oscilloscope. Software compares the intensity of the two pulses and the normalized difference is recorded. Scanning the pulse shape produces a spectrum, scanning the mirrors creates an image. The SRS process is explained and contrasted with the two beam implementation diagrammatically on the right. The Raman transition probability, $P_{a\to b}$, can be controlled by adjusting the phase, $\phi(\omega)$, in the broadband case. BS: beam splitter, DM: dichroic mirror, fs: femtosecond.

identical in energy and spectrum but not spectral phase, is created, and the two pulses are focused on the sample. If a compound of interest is on the surface, there will be a transfer of photons between the two halves of the spectrum of the first pulse leading to SRG and SRL. However, this transfer does not happen for the second pulse because it has a different phase that tunes it out of resonance. The diffusely reflected laser scatter from both pulses is collected, and the relative intensity of the two spectral halves of each pulse is recorded with 1 GHz amplified photodiodes and digitized with an oscilloscope (Lecroy, Waverunner 610zi). The SRL and SRG are computed, and the experimental components are synchronized to allow image acquisition at the maximum rate allowed by the pulsed laser, here 1 kHz. The reference pulse is required to prevent optical characteristics (absorptivity and/or reflectivity) of the target from contributing to the signal. Furthermore, SB-SRS eliminates contributions from laser power fluctuations that otherwise limit the sensitivity of the technique (see Supplementary Information S1 in Ref. 22). The combination of selectivity and the intrinsic reference result in a robust method to detect trace quantities of explosives on a wide variety of real-world chemically complex surfaces without the need for a spectrometer.

Selective excitation of particular Raman modes using a phase shaped femtosecond laser was demonstrated by Weiner *et al.* using prefabricated periodic spectral phase masks and time domain transient grating detection.[23] Silberberg's group used a computer controlled spatial light modulator and a sinusoidal spectral phase to perform single beam CARS microscopy,[24] and the Dantus group utilized selective excitation in the first single-beam CARS standoff measurements.[9] Conceptually, quantum interference between different pathways of excitation available within the laser bandwidth leads to selective excitation of a particular vibrational mode, determined by the spectral phase.[24] Here we use a pair of displaced parabolic phase functions, which are the frequency analog to a pair of time-displaced chirped pulses that have been shown to cause selective vibrational excitation.[25] Here, selective excitation provides the spectroscopic resolution for single-beam measurements of SRG and SRL. Figure 2, presents details of the specific implementation. Recent analysis by Rahav and Mukamel describing

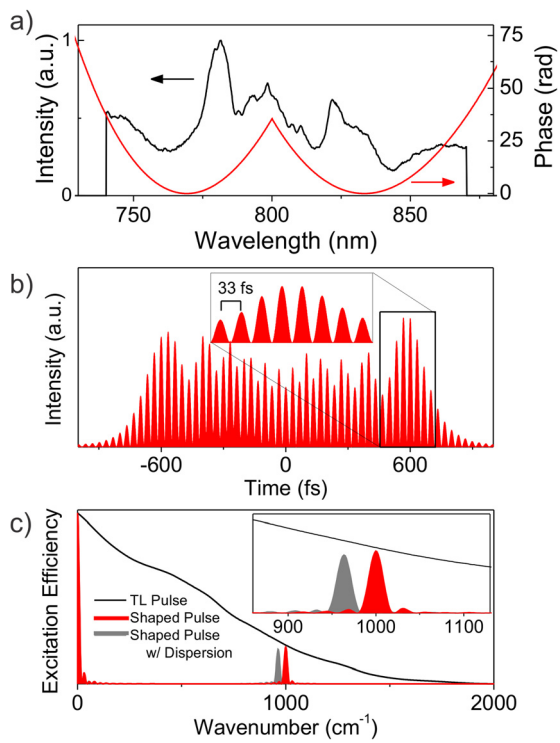

FIG. 2. Selective Raman excitation. (a) Experimental laser spectrum and phase. (b) Simulated time domain intensity profile. (c) Calculated excitation efficiency. The selective excitation phase is designed for a 1000 cm^{-1} Raman transition and the supercontinuum laser spectrum is cut to cover 2000 cm^{-1} shift, which is optimal in this example.[22] The resultant time domain intensity profile consists of a long pulse train with a period of 33.3 fs. The SRS excitation spectrum (c) has a resolution of ~25 cm^{-1}, yet equivalent excitation efficiency as a transform limited pulse (TL). The peak of excitation shifts by ~40 cm^{-1} with the application of 300 fs^2 of group delay dispersion.

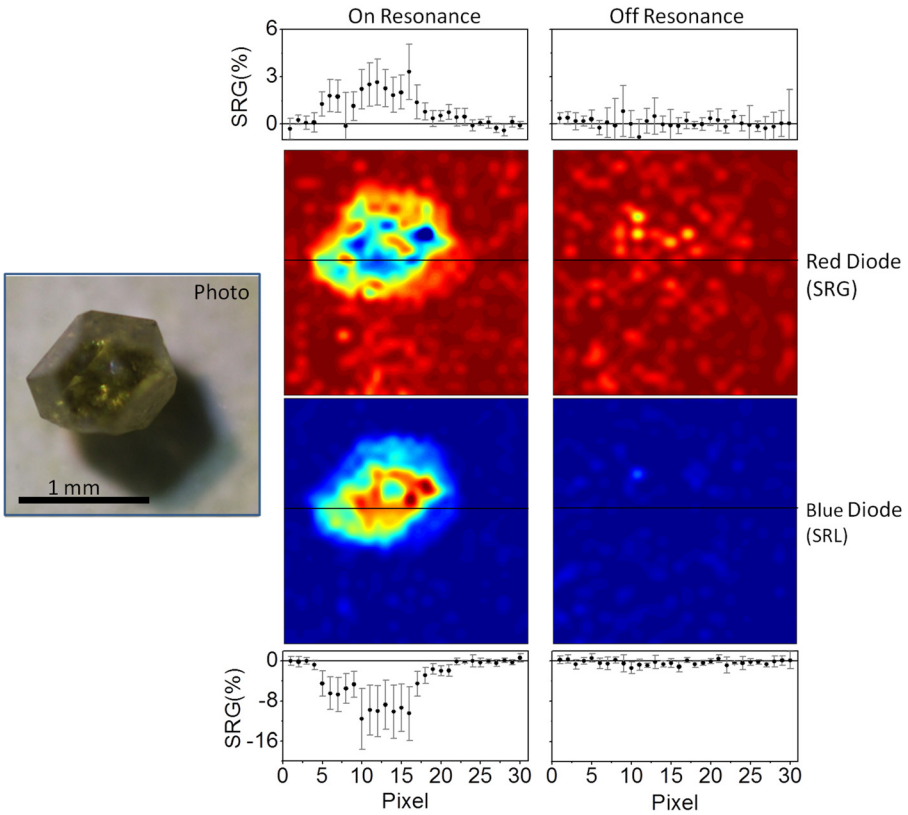

FIG. 3. Chemical images of a diamond on adhesive paper acquired with 10 laser pulses per pixel. Both SRG (top row images) and SRL (bottom row images) are detected simultaneously. With the pulse shape tuned to 1360 cm^{-1} (on resonance), the diamond is clearly visible. Off resonance (1050 cm^{-1}), only noise is observed. The insets show the data acquired along the black line in the images. The statistical analysis of the data includes error bars corresponding to 1 standard deviation of the mean, note this is a zero-background method.

heterodyne CARS from the material's perspective using scattering theory provides an intuitive framework to describe features of the broadband SRS measurement,[26,27] a more complete theoretical formulation is provided in Supplemental Section S2 of Ref. 22. Recently, broad bandwidth sources taking advantage of chirped pulse selective excitation[25] have been used for SRS microscopy.[28–30]

We find that single-beam SRS allows us to obtain 3:1 or better signal-to-noise ratio with few (<10) laser pulses. We are able to obtain a complete Raman spectrum in a few seconds by scanning the selective phases using the computer controlled pulse shaper (see Supplemental Section S3 of Ref. 22). However, the best application of SB-SRS is to quickly monitor the intensity of one or a few vibrational resonances for chemical imaging as in SRS microscopy.[18] Figure 3 shows such an image, created by raster scanning a "post-it" note with a small diamond placed on the adhesive portion. With 10 laser shots per pixel, a satisfactory chemical image is created using SRG or SRL. With the phase tuned off resonance, only noise is visible. This shows that SB-SRS is only sensitive to chemical information, and bright field features only manifest as a change in noise magnitude. The images also have no background, as shown in the line scans; thus, SB-SRS can be used for detection in addition to image contrast.

Figure 4 shows SB-SRS chemical images of plastic and cotton surfaces. In samples (a) and (b), 100 μg of dissolved ammonium nitrate (NH_4NO_3) was sprayed non-uniformly over a 1 cm^2 area and allowed to dry. In (c), trinitrotoluene (TNT) microcrystals were deposited in the same concentration by dry transfer. From the photos, the samples consist of collections of micro-particles or thin residues. Zero background chemical images are obtained from these surfaces with 20 laser shots per pixel.

It is challenging to uniformly deposit smaller quantities than those present in Figure 4. However, by careful observation of an adhesive paper substrate before and after

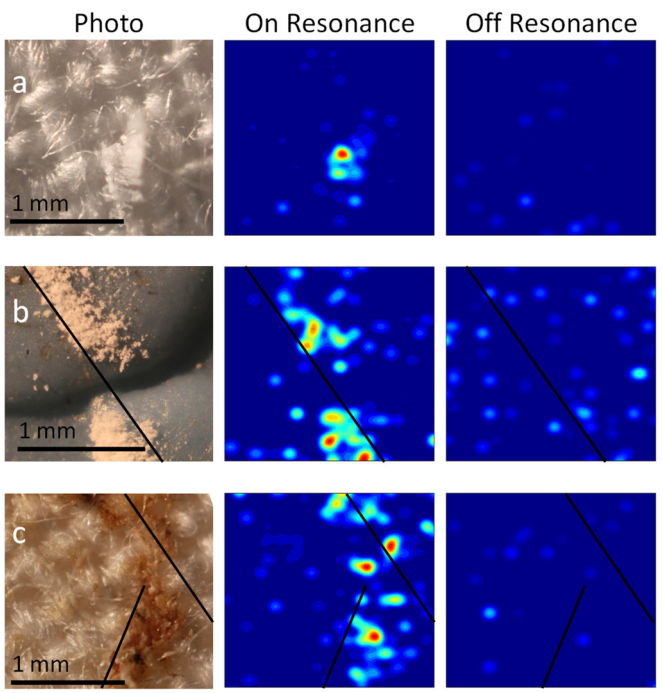

FIG. 4. Standoff SRS images of NH_3NO_4 on cotton (a) and blue textured plastic (b) and TNT on cotton (c). The sample distribution on each substrate corresponds to ~100 $\mu g/cm^2$, although the local concentration is higher. With 20 laser shots per pixel in the 30 × 30 images, the distribution of the analyte is recorded by observing SRL. Statistics were used to eliminate points less than 0.8 standard deviations of the mean above zero. The black lines are guides to the eye. On (off) resonance is 1043 cm^{-1} (950 cm^{-1}) for NH_4NO_3 and 1360 cm^{-1} (1043 cm^{-1}) for TNT. Data for (a) and (c) were collected at 10 m and (b) at 7.5 m.

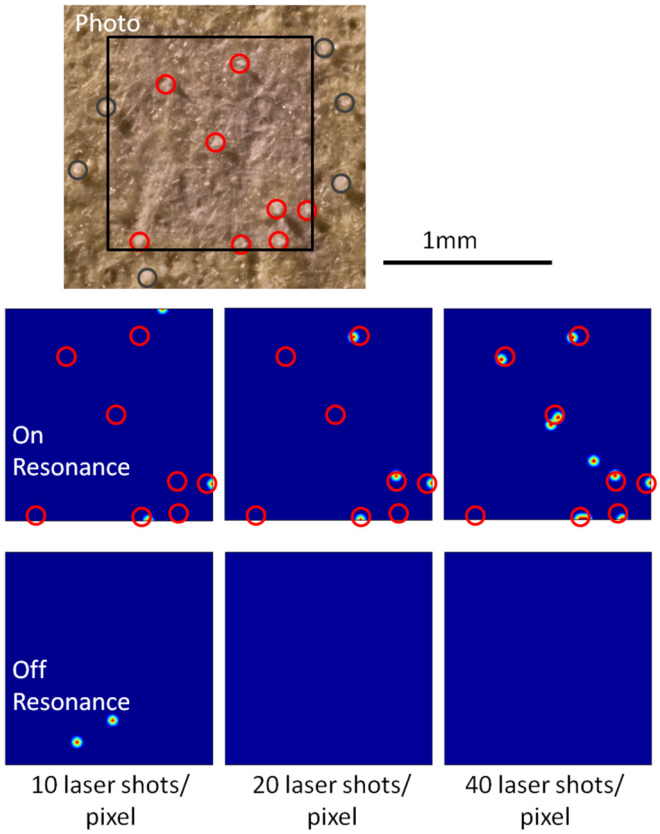

FIG. 5. Detection of single micro-particles of NH_4NO_3 deposited on an adhesive paper. The circles identify the micro-particles deemed to be the largest (judged by the shadow cast upon side illumination). In the chemical images, points less than 1.5 standard deviations of the mean above zero are equated to zero, all other points given a value of one. This analysis allows an occasional false positive, but with 20 laser pulses half of the circled particles are identified. A sieve (75 μm), was used to ensure small particle size. Image: 30 × 30 (0.9 s per single shot image on the 1 kHz system). Signal collected at 10 m.

deposition, one can identify single micro-particles of NH_4NO_3. Figure 5 shows that a majority of the largest particles are identified with just 20 laser shots. The zero level background and statistics obtained from multiple laser shots provide a powerful approach with which to claim "yes or no" detection. The circled particles' diameters are ~25–50 μm with calculated masses between ~15 and 100 ng. Imaging 15 ng particles in a 1.5 mm^2 area is equivalent to ~1 $\mu g/cm^2$; single particles would also be detected on 1 cm^2 areas supporting a claim of sub-microgram per cm^2 sensitivity.

In comparison to CARS, SB-SRS offers several advantages. The absence of non-resonant background makes SB-SRS an ideal "yes or no" detection approach. The process scales linearly with concentration; thus, the signal from minority constituents is less likely to be overwhelmed by other materials. Note that SB-SRS requires no spectrometer. In terms of speed, the images presented here were acquired at a rate that is two orders of magnitude faster than those previously attained with standoff CARS imaging and a similar setup.[14]

An interesting aspect of SB-SRS is that the signal is measured by monitoring the diffusely reflected laser light, which is quite intense and easily collected with small optics at large distances. For detection distances less than 10 m, the signal was attenuated to prevent saturation of the simple photodiodes used to detect the SB-SRS signal. This suggests that SB-SRS could be very useful for greater standoff distances, especially since the implementation is robust against beam pointing instabilities due to the short delay of the reference. As with SRS microscopy, the fundamental sensitivity limit of SB-SRS is related to the photon number shot noise,[31] about 10^{-5} per pulse with a 2 in lens at 10 m. The noise level of our implementation is significantly above this level, and the technique is presently limited by the accumulated instrument noise (~0.5% rms).

We have introduced a standoff detection and imaging method, SB-SRS, which uses the non-linear process of stimulated Raman scattering. Coherent control of Raman transitions provides the chemical specificity for the single beam method, and time multiplexing enables single shot implementation. With 10 mW of laser power in the near IR, we can detect a single ~15 ng particle of an explosive simulant within 20 ms on a number of "real-world" delicate substrates such as paper, clothing, and plastic. The speed, sensitivity, and robust performance on chemically complex substrates make this technique one of the most promising methods for standoff detection of trace quantities of explosives. A scientific research laser was used in this initial implementation. Based on advances in photonics over the past 10 years, it is fair to assume a compact and industrial type of laser with the desired characteristics should be available soon to make this approach widely available.

Funding for this research was provided by the department of Homeland Security, Science and Technology Directorate, under Contract No. HSHQDC-09-C-00135 (Dr. Michael Shepard, Program manager), administered by The John Hopkins University, Applied Physics Laboratory (Dr. Robert Osiander and Dr. Jane M. Spicer Program Managers). The samples deposited on cotton and plastic were provided by the Applied Physics Laboratory.

[1]D. S. Moore, Rev. Sci. Instrum. **75**, 2499 (2004).
[2]D. S. Moore, Sens. Imaging Int. J. **8**, 9 (2007).
[3]S. Wallin, A. Pettersson, H. Östmark, and A. Hobro, Anal. Bioanal. Chem. **395**, 259 (2009).
[4]U. Willer and W. Schade, Anal. Bioanal. Chem. **395**, 275 (2009).
[5]J. C. Carter, S. M. Angel, M. Lawrence-Snyder, J. Scaffidi, R. E. Whipple, and J. G. Reynolds, Appl. Spectrosc. **59**, 769 (2005).
[6]A. Pettersson, S. Wallin, H. Östmark, A. Ehlerding, I. Johansson, M. Nordberg, H. Ellis, and A. Al-Khalili, Proc. SPIE **7664**, 76641K (2010).
[7]A. Tripathi, E. Emmons, P. Wilcox, J. Guicheteau, D. Emge, S. Christesen, and A. Fountain, Appl. Spectrosc. **65**, 611 (2011).
[8]D. Pestov, R. K. Murawski, G. O. Ariunbold, X. Wang, M. Zhi, A. V. Sokolov, V. A. Sautenkov, Y. V. Rostovtsev, A. Dogariu, Y. Huang, and M. O. Scully, Science **316**, 265 (2007).
[9]H. Li, D. Harris, B. Xu, P. Wrzesinski, V. Lozovoy, and M. Dantus, Opt. Express **16**, 5499 (2008).
[10]O. Katz, A. Natan, Y. Silberberg, and S. Rosenwaks, Appl. Phys. Lett. **92**, 171116 (2008).
[11]A. Portnov, S. Rosenwaks, and I. Bar, Appl. Phys. Lett. **93**, 041115 (2008).
[12]H. Li, D. A. Harris, B. Xu, P. J. Wrzesinski, V. V. Lozovoy, and M. Dantus, Appl. Opt. **48**, B17 (2009).
[13]D. S. Moore, S. D. McGrane, M. T. Greenfield, R. J. Scharff, and R. E. Chalmers, Anal. Bioanal. Chem. **402**, 423 (2012).
[14]M. T. Bremer, P. J. Wrzesinski, N. Butcher, V. V. Lozovoy, and M. Dantus, Appl. Phys. Lett. **99**, 101109 (2011).

[15]A. Natan, J. M. Levitt, L. Graham, O. Katz, and Y. Silberberg, Appl. Phys. Lett. **100**, 051111 (2012).
[16]Y. R. Shen, *The Principles of Nonlinear Optics* (Wiley-Intersci., New York, 1984), p. 146.
[17]E. Ploetz, S. Laimgruber, S. Berner, W. Zinth, and P. Gilch, Appl. Phys. B **87**, 389 (2007).
[18]C. W. Freudiger, W. Min, B. G. Saar, S. Lu, G. R. Holtom, C. He, J. C. Tsai, J. X. Kang, and X. S. Xie, Science **322**, 1857 (2008).
[19]B. G. Saar, C. W. Freudiger, J. Reichman, C. M. Stanley, G. R. Holtom, and X. S. Xie, Science **330**, 1368 (2010).
[20]Y. Ozeki, Y. Kitagawa, K. Sumimura, N. Nishizawa, W. Umemura, S. Kajiyama, K. Fukui, and K. Itoh, Opt. Express **18**, 13708 (2010).
[21]Y. Coello, V. V. Lozovoy, T. C. Gunaratne, B. Xu, I. Borukhovich, C. Tseng, T. Weinacht, and M. Dantus, J. Opt. Soc. Am. B **25**, A140 (2008).
[22]See supplementary material at http://dx.doi.org/10.1063/1.4817248 for additional information, including noise reduction efficacy, theoretical description of the process, and example spectra created with the technique.
[23]A. M. Weiner, D. E. Leaird, G. P. Wiederrecht, and K. A. Nelson, Science **247**, 1317 (1990).
[24]N. Dudovich, D. Oron, and Y. Silberberg, Nature **418**, 512 (2002).
[25]E. Gershgoren, R. A. Bartels, J. T. Fourkas, R. Tobey, M. M. Murnane, and H. C. Kapteyn, Opt. Letters **28**, 361 (2003).
[26]S. Rahav, O. Roslyak, and S. Mukamel, J. Chem. Phys. **131**, 194510 (2009).
[27]S. Rahav and S. Mukamel, Proc. Natl. Acad. Sci. **107**, 4825 (2010).
[28]E. R. Andresen, P. Berto, and H. Rigneault, Opt. Lett. **36**, 2387 (2011).
[29]H. T. Beier, G. D. Noojin, and B. A. Rockwell, Opt. Express **19**, 18885 (2011).
[30]D. Fu, G. Holtom, C. Freudiger, X. Zhang, and X. S. Xie, J. Phys. Chem. B **117**, 4634 (2013).
[31]Y. Ozeki, F. Dake, S. Kajiyama, K. Fukui, and K. Itoh, Opt. Express **17**, 3651 (2009).